Automatic Insulator Detection for Power Line Using Aerial Images Powered by Convolutional Neural Networks

Automatic Insulator Detection for Power Line Using Aerial Images Powered by Convolutional Neural Networks

Jicheng Tan[1, *]

[1]School of Hefei University of Technology, Hefei, Anhui 230009, China.

[*]Corresponding author's e-mail: tanjicheng@mail.hfut.edu.cn

Abstract. The inspection and fault diagnosis of power transmission line via aerial images is becoming widely used in smart grids and electrical power systems. However, the accuracy of detecting objects with complicated backgrounds still remains an important challenge in the defect detection system. In this article, a deep-learning based method is presented to realize the automation of insulator fault detection. In the proposed approach, the insulator localization network based on Single Shot Multibox Detector (SSD), a one-stage detecting backbone, is utilized to extract multi-level features and make predictions in order to determine the insulator situation in the aerial images. Additionally, Densely Connected Convolutional Networks (DenseNet) is newly introduced to strengthen the insulator detecting system's classification ability. To address the data scarcity problem, a two-stage data augmenting strategy is also applied. The first stage is mainly based on the image combination, while the second stage includes random affine transformation, Gaussian blur, brightness and contrast transformation, and salt-and-pepper noise. The insulator detection network and the classification network precisions of the proposed method have reached 0.95 and 0.98 using the text dataset, respectively. The results have shown that the proposed method can ensure robustness and accuracy during insulator detection.

1. Introduction

Power transmission line is one of the most essential parts in delivering electricity in power grids. The reliability of the transmission line directly determines the capacity and safety of the power supply. According to earlier researches, insulator defects in the transmission lines account for the highest ratio in power transmission accidents [1]. Meanwhile, insulators are extremely necessary assembly units in power delivery that can achieve electrical insulation and mechanical fixation in order to ensure the security of wires. Therefore, power line insulator defects detection makes a great contribution to maintain stability in the power system. The traditional methods, mainly based on manual operations, like physical patrol or helicopter investigation [2], extremely restrict the quick-acting of detection and effectiveness of insulator protection. In addition, the traditional inspection generally fails to handle the cluttered background condition, for it can merely function in certain environments, angles, and illuminations [1].

In recent years, in order to enhance the efficiency and security of insulator defect detection, researchers have been developing the automatic inspecting power transmission system based on aerial platforms, such as unmanned aerial vehicles (UAVs) [3]. The inspecting system usually consists of two sections: image acquisition and defect detection. Normally, a camera is mounted on the aerial platform and captures the images with information of certain objects (insulators). Those images will then be sent as initial data to the ground monitoring centers for further analysis and fault diagnosis [4]. Nevertheless,

Miao et al. [3] introduced that insulators were typically located in various cluttered backgrounds, which generates the accuracy of insulators localization to be affected by numerous unfavorable factors to some certain extent,. Moreover, Jiang et al. [4] proposed that regional differences and data confidentiality caused by various scenes and components would lead to the inspection of region independence and data scarcity. Tao et al. [1] raised an issue that there was still no authoritative, comprehensive evaluation benchmark for insulator inspection has been established. In brief, the insulator inspection based on aerial platforms remains challenging tasks.

Narrowing down the main range of mentioned challenges, we can classify them into three categories: insulator localization, fault detection, and lack of data. Several studies have investigated the orienting method via exterior features, including color, shape, and texture. [3]. Zhao et al. [5] presented a method that utilized Orientation angle detection and binary shape (OAD-BSPK) to simulate multiple insulator locations with different angles. Wang et al. [6] applied an inspecting scheme that integrated shape, color, and texture to reduce the effects caused by the complex surroundings. Wu et al. [7] proposed a texture segmentation algorithm to extract and optimize the texture features of insulators from aerial images. Zhang et al. [8] adopted a connected component analysis method dedicated to the tempered glass insulator identification via several typical colorific elements. Oberweger et al. [9] introduced an insulator detector based on a circular descriptor and a noise-tolerant voting scheme, leveraging the extracted difference of Gaussians (DoG) key-points to recognize the repetitive geometric structure and a particular circular shape feature of insulator cap. However, the overwhelming majority of the solutions mentioned above are limited by environment circumstances, for they might focus on certain backgrounds or certain types of insulators.

As for fault detection, the mainstream works have mentioned utilizing deep learning algorithms to execute automatic defect inspection. Murthy et al.[10] applied a method that combined the wavelet transform, multi-resolution analysis (MRA) technique, and support vector machine (SVM) to diagnose and capture the small faults of the insulator. Zhao et al. [11] introduced a multi-patch feature extraction method based on a convolutional neural networks (CNN) model. Nguyen et al. [2] combined Single Shot Multibox Detector (SSD) [12] and deep Residual Networks (ResNets) [13] as a multi-stage component detection to classify and detect small components and faults. Tao et al. [1] leveraged cascading CNNs that recognized the insulator defects by Defect detector network (DNN), utilizing the Region proposal network (RPN) approach to localize the insulator previously.

Several researches have presented effective methods to achieve data augmentation mainly based on affine transformations, while elastic deformations [14], Gaussian Blur [1,2], insulator segmentation, and background fusion [1] were also ingeniously implemented. Furthermore, Miao et al.[3] indicated a two-stage fine-tuning method based on existed COCO model, which allowed them to obtain an adequate dataset from the outset.

Inspired by related work, this paper attempts to combine the existed methods and optimize the defect detecting process. An autonomous insulator detection CNN architecture based on the SSD, DenseNet [15], and a two-stage data augmentation strategy is developed. A dataset was created with various background images such as grass, mountain, river, high-voltage tower, and tree in the first stage. And image combination is applied to synthesize insulator images, including normal insulator and defect insulator, to the background images. In the second stage, random affine transformation, Gaussian blur, brightness and contrast transformation, and salt-and-pepper noise are used to strengthen the synthesized dataset. After processing the data, the classification and detection backbone based on the SSD network is utilized to extract multi-stage features from the images and identify the insulator components and defects. The detected portion is afterwards inputted into the classification network based on DenseNet to determine the category. Due to the less possibility of being affected by negative samples, this approach can accurately localize the object and indicates great robustness and effectivity.

The rest of this paper is organized as follows. In Section Two, the system framework of this proposed insulator defect detecting approach and brief introductions of the principles of related methods are described. The experimental results of various conditions and corresponding analysis are presented in Section Three. Section Four concludes the results, and future improvement methods are also discussed.

2. Methodology

2.1. System framework

The proposed deep-learning-based insulator defect detecting approach consists of three parts: dataset processing, training architecture based on SSD network and DenseNet classification network, and insulator detection. The flow chart of the entire insulator inspecting process is shown in Figure 1. Firstly, the raw images of insulators on the power transmission lines will be captured by aerial platforms like UAVs. The images will be preprocessed through a two-stage augmenting procedure to transform into the enhanced dataset for further training. During the training process, the SSD network is utilized for training the specific insulator detection model. Different from antecedent deep learning backbones, the DenseNet, considered as an optimized version of ResNet, was introduced to localize and classify normal and defect components, which performed excellent accuracy and robustness. The well-trained model will be implemented in subsequent insulator inspection.

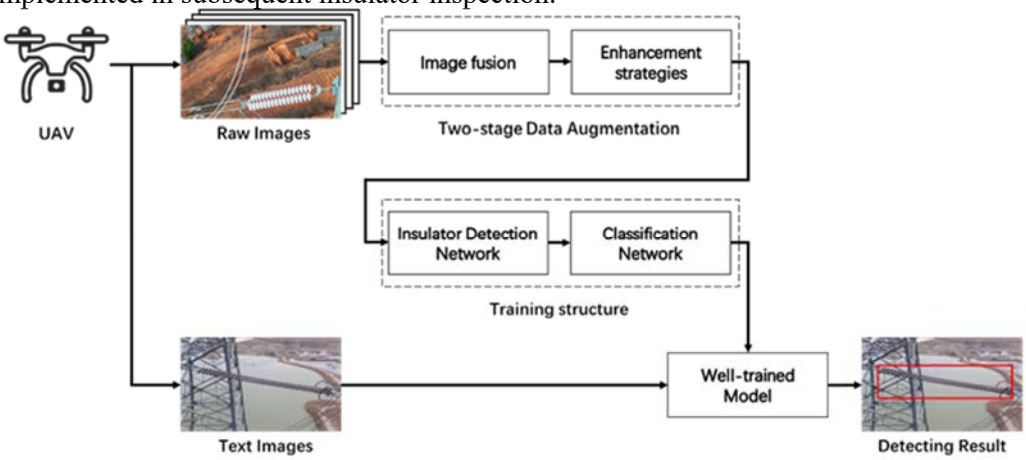

Figure 1. Insulator inspecting process.

2.2. Data augmentation

The initial datasets, including insulator conditions, are too small for effective training without overfitting, the appropriate expanding measure was essential. On the one hand, the enhancement can strengthen the robustness of training results. On the other hand, the object segmentation and background fusion method can decrease the influence of negative samples, which guarantees the training effect. The brief schematic diagram of the data augmenting procedure is shown in Figure 2.

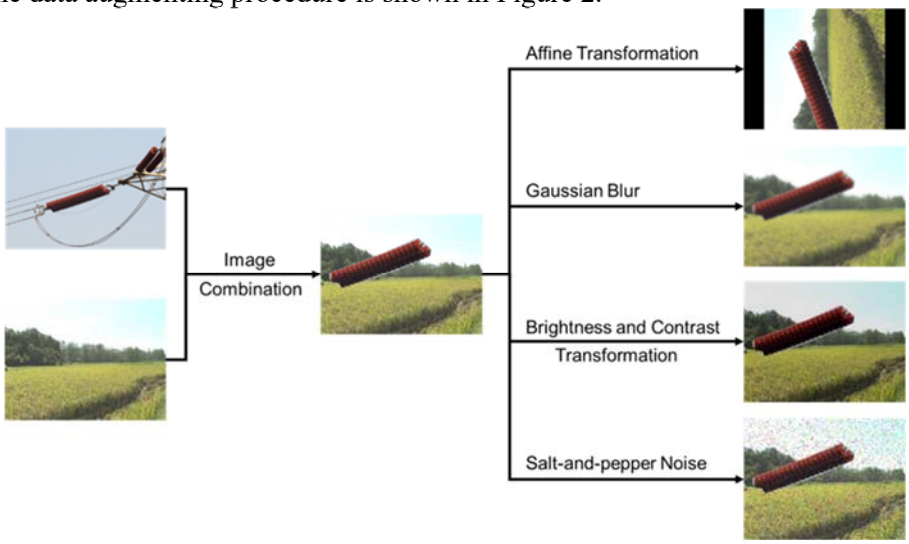

Figure 2. Data augmenting procedure.

2.3. DL-based Training Architecture

The proposed training architecture mainly includes two networks: an insulator localization network based on the SSD network and a classification network based on DenseNet. The former network spots the position of insulators, and the latter determines the concrete category of the detected insulators. In this model, the end-to-end training is adopted, and the classification results are accurate even for images with relatively small resolution. Different from the two-stage training method, such as RPN (Region Proposal Network), this approach enhances the inference speed and avoids heavy classification subnet. The whole training structure is shown in Figure 3.

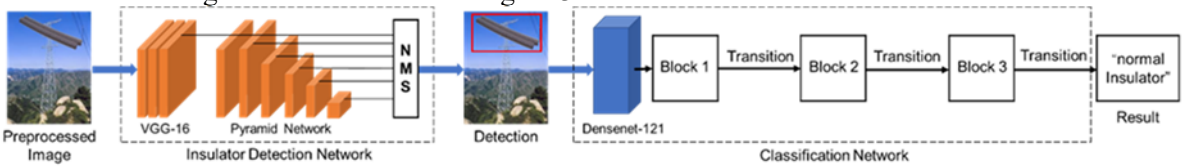

Figure 3. Training architecture.

2.3.1. Single shot muiltbox detector

SSD is a bounding box based on a forward-spreading CNN network, which produces a series of fixed-size bounding boxes, and the possibility of object instances contained in each box, namely score. A non-maximum suppression is implemented afterwards to get the final predictions. The SSD network structure can be divided into two parts: a base network and a pyramid network. The base network is the first four layers of the VGG-16 network, while the pyramid network is a simple convolutional network with gradually smaller feature maps. The entire training procedure and principle of the SSD network are as follows:

Matching each ground truth box with the default box with the largest jaccard overlap ensures that each ground truth has a corresponding default box. And matching each default box with any ground truth, a ground truth box may correspond to multiple default boxes as long as the jaccard overlap of both is greater than a certain threshold. Jaccard overlap is calculated:

$$J(A,B) = \frac{|A \cap B|}{|A \cup B|} = \frac{|A \cap B|}{|A|+|B|-|A \cap B|} \tag{1}$$

The loss function of the SSD algorithm is divided into two parts: the calculation of the confidence loss of the corresponding default box with respect to the target category and the corresponding position regression.

$$L(x,c,l,g) = \frac{1}{N}\left(L_{conf}(x,c) + \alpha L_{loc}(x,l,g)\right) \tag{2}$$

Where N is the number of default boxes matched to ground truth, and the α parameter is used to adjust the ratio between confidence loss and location loss, default α = 1.

Since feature maps of different layers correspond to different receptive fields on the original drawing, the size of the default box generated in different layers is actually different. When generating the default box, a series of concentric default boxes are produced on each point of the feature map (then the coordinates of the center point are multiplied by step, which is equivalent to mapping back to the original location from the feature map) and m (here m = 6 by virtue of 6 selected layers) different feature maps are used for prediction. The scale value of the feature map at the bottom layer is s_{min}=0.2, while that at the top layer is s_{max}=0.9. The other scale of the default box can be calculated by the following formula:

$$s_k = s_{min} + \frac{s_{max}+s_{min}}{m-1}(k-1) \tag{3}$$

The aspect ratios of the default box are {1, 2, 3, 1/2, 1/3}. For aspect ratio = 1, an additional default box is added, and the scale of the box is:

$$s'_k = \sqrt{s_k s_{k+1}} \tag{4}$$

For each default box, the width and height are calculated as follows:

$$w_k^a = s_k\sqrt{a_r} \tag{5}$$

$$h_k^a = \frac{s_k}{\sqrt{a_r}} \tag{6}$$

Additionally, the center point coordinates of default Box are:

$$\left(\frac{i+0.5}{|f_k|}, \frac{j+0.5}{|f_k|}\right) \tag{7}$$

In the back-end of the model, hard negative mining and data augmentation are designed to speed up network convergence. The approaches above guarantee the accuracy and speed of detecting insulators.

2.3.2. DenseNet

In order to solve the vanishing gradient problem, many structures have been proposed, such as ResNet, Highway Networks, Stochastic depth. Despite the differences in network structure, it is not difficult to change the core idea of creating a straight-through route from the top layer to the bottom layer. Compared to ResNet, DenseNet proposes a more radical mechanism of dense connection: All layers are connected to each other. Each layer accepts all layers before it as its additional input, specifically.

In order to achieve the above-mentioned transfer of information from all layers, the dense block structure is used in DenseNet. In previous convolutional neural networks, L layers would contain L connections. However, the L layers will have $\frac{1}{2}L(L+1)$ connections in DenseNet, which is called a full connection. The output of the L layer can thus be expressed by the following formula:

$$x_l = H_l([x_0, x_1, \dots, x_{l-1}]) \tag{8}$$

Where $H_l(x)$ above represents a non-linear transformation function, a combinatorial operation that may include a series of BN (Batch Normalization), ReLU, pooling, and convolutional operations.

The connection mode adopted by dense block leads to more efficient transmission of features and gradients and easier training of the network. The main reason for gradient loss is that the input and gradient information are passed between many layers, which is related to the computational mechanism of feedforward and feedback operations. Nevertheless, a dense block connection is equivalent to a direct connection between each layer and input and loss, which mitigates gradient loss.

However, the features extracted at each layer of the neural network correspond to a nonlinear transformation of the input data. With the increase of depth, the complexity of the transformation gradually increases, giving rise to heavier computation and larger memory occupancy, simultaneously higher possibility for overfitting. To avoid this, the bottleneck layer and transition layer are introduced in the DenseNet network. The main purpose of the bottleneck is to reduce the number of channels for dimensionality reduction and to reduce the amount of computation, while the transition layer is applied to alleviate the dimensionality of the feature map and to decrease the number of channels for dimensionality reduction. Moreover, all layers of the dense block output k features after convolution, which means the resulting feature map contains k channels, or k convolution kernels. k is called growth rate in DenseNet. Therefore, better performance can be achieved by using a smaller k. The key lies in the reduction of computation and the reuse of features in each layer. k in DenseNet requires merely a few features to be learned per layer, resulting in a significant reduction in the number of parameters and computations.

In conclusion, the dense block establishes connections between layers, fully leveraging the features, and further mitigating the gradient loss problem. Bottleneck layer, translation layer, and small growth rate result in a narrower network with fewer parameters, which suppress the overfitting and reduce the computation. These advantages allow DenseNet to remain accurate in classifying insulators under circumstances where the difference between normal and faulty insulators in aerial images is subtle, and the data is not extensive enough.

3. Experiment and result

In this section, the performance of the proposed method was evaluated by using an insulator dataset from real scenes, including several backgrounds considered above. Firstly, the process of preparing the experimental dataset and the environment configuration of the experiment are described. Secondly, the parameter setting and evaluation criteria are displayed. Furthermore, this paper experiments with the detection performance of the method through two approaches. First, the detection accuracy of the method is evaluated by locating insulators in different backgrounds. Secondly, the performance of the

insulator detection network and classification network is examined through a series of evaluation metrics. Afterwards, the results are counted and analyzed accordingly. Finally, some of the detection results are presented in the form of images.

3.1. Dataset preparation and environment configuration

The training dataset used in this experiment consists of 1308 images, including 86 original images from the Internet and 1222 composite images. The original images cover various background environments where insulators may appear, out of which 14 contain grass, 15 contain mountains, 13 contain rivers, 14 contain high-voltage towers, 14 contain trees, and 16 contain cluttered background. In addition, the 1308 images contain 1122 positive samples (images containing normal insulators) and 186 negative samples (images containing defective insulators). The positive and negative samples, except for the 86 original images, are fused with one or more normal or defective insulators through data-enhancement, respectively.

The proposed experiments are conducted in Pytorch 1.3 deep learning framework, executed on the computer equipped with Intel Core i7 series CPU, TITAN Xp with GPU memory of 8 GB, and 32GB RAM under Windows10 operating system.

3.2. Parameter setting and evaluation criteria

The test dataset applied in the experiment consisted of 400 images, which come from the web and partly referred from the Chinese power line insulator dataset utilized in Tao[1]'s work. Some of the samples were also obtained by means of data augmentation. The parameter settings of data reinforcement are presented in Table 1

Table 1.Parameter setting of data augmentation.

Parameter	Value
rotation range	60,120,150,210,240
noise range	5%
Gaussian kernel size	5*5
brightness fluctuation range	±60
contrast fluctuation range	0.7-1.3

For the training network, the insulator detection network is based on the SSD network, and the pre-training model of VGG-16 is adopted. The classification network is based on the DenseNet network and utilizes the DenseNet-121 pre-training model. The training parameters for the insulator detection network and the classification network are shown in Table 2 and Table 3.

Table 2. Parameter setting of insulator detection network.

Parameter	Value
Batch size	4
IoU threshold	0.5
Epoch	60
Learning rate	0.001

Table 3. Parameter setting of classification network.

Parameter	Value
Batch size	4

Epoch	100
Num classes	2
Learning rate	0.001
Weight decay rate	0.0005
Momentum rate	0.9

In order to evaluate the performance of the detection method, the following metrics are introduced in this paper: $Precision$, $Recall$, $Accuracy$, and F_1. $Precision$ is for the predicted results, representing the probability of actually being a positive sample out of all the samples that were predicted to be positive. $Recall$ is for the original sample, meaning the probability that a positive sample will be predicted out of all positive samples. $Accuracy$ is the percentage of the total sample that is correctly predicted. F_1 is a measure that considers both accuracy and recall to achieve the highest possible balance between the two at the same time. Higher evaluation values lead to better performance.

$$Precision = \frac{T_P}{T_P+F_P} \tag{9}$$

$$Recall = \frac{T_P}{T_P+F_N} \tag{10}$$

$$Accuracy = \frac{T_P+T_N}{T_P+T_N+F_P+F_N} \tag{11}$$

$$F_1 = \frac{2*Precision*Recall}{Precision+Recall} \tag{12}$$

where T_P (True Positive) refers to the number of insulators present in the image and correctly detected, and F_P (False Positive) denotes the number of insulators not present in the image but detected. Thus $T_P + F_P$ is the total number of detected insulators. F_N (False Negative) is the number of insulators present in the image but not detected. Thus, $T_P + F_N$ is the actual number of insulators.

Whether each model should be predicted as T_P, T_N (True Negative), F_P or F_N is defined by a parameter called IoU (intersection-to-unity ratio), which is the intersection ratio between the target window generated by the model and the original marker window. In the target detection task, if the IoU value of the rectangular box output by the model and the manually marked rectangular box is greater than a certain threshold (where IoU threshold=0.5), the model is considered to have output the correct one.

3.3. Results

3.3.1. Insulator detection in various scenes

The 400 pictures used for testing cover several scenarios mentioned in the text inwhich the insulators probably occur. Each sample contains multiple normal and defective insulators. Figure 4 shows that the detection accuracies of the positive and negative samples are 0.99 and 0.88 for the grass scene, 0.97 and 0.84 for the mountain scene, 0.94 and 0.91 for the river scene, 0.96 and 0.92 for the high voltage tower scene, and 0.99 and 0.80 for the tree scene. It can be seen that the detection accuracy of defective insulators is generally lower than that of normal insulators. In addition, the detection accuracy of both normal and faulty insulators can be maintained at a high level regardless of the scenario, which shows that the proposed method can effectively overcome the interference brought by different scenarios and possess well-detected performance.

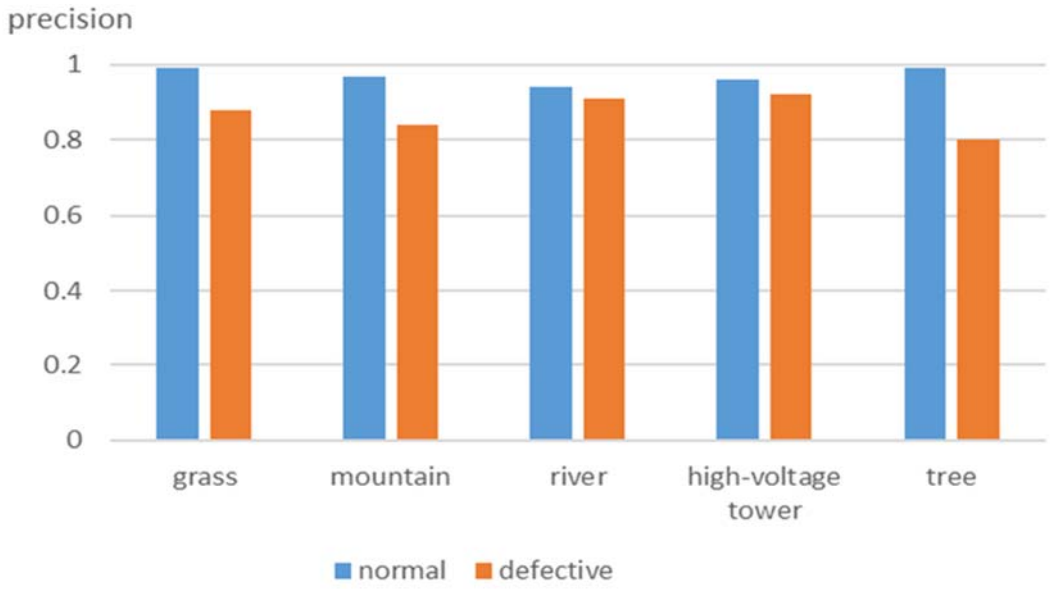

Figure 4. Precision results analysis of insulator detection in different scenes.

3.3.2. Performance of the training architecture

Table 4 shows the training performance of the insulator detection network and the classification network. When the epoch reaches 60, the value of precision of both networks reaches 0.95 and 0.98, while that of recall achieves 0.92 and 0.96, that of accuracy gets 0.89 and 0.92, and that of F1 value reaches 0.93 and 0.97. It can be seen that the classification network generally has a higher index of detection performance evaluation than the insulator detection network. This is because the main function of the classification network is to determine the category of insulators, whereas the function of the detection network is not only to determine the category but also to identify the specific location of insulators. In addition, the average running time for each step of the insulator detection network has reached 0.1 seconds, while the classification network achieved 0.05 seconds, demonstrating the efficiency of the method.

Table 4. Performance of training architecture

Network	Precision Rate	Recall Rate	Accuracy Rate	F_1 Rate	Testing Speed
Insulator Detection Network	0.95	0.92	0.89	0.93	0.1
Classification Network	0.98	0.96	0.92	0.97	0.05

3.3.3. Result exhibition

To manifest the well-detecting results of the method, several pictures used for testing are shown in Figure5 and Figure 6. Figure 5 shows the results of the insulators inspected in each background. Each insulator detected is marked with a rectangular box with the confidence level located at the top left of the box. As can be seen, the detection performance of the proposed method is significant in different backgrounds. In Figure 6, the results of partial detection of normal and faulty insulators are shown, and each detected insulator is also bounded by a rectangular box, where the normal insulators are framed by yellow boxes. The defective insulators are framed by red boxes. The confidence level, as well as the category label of the insulator being detected, is located at the top of the box. Figure 6 shows that the characteristics

of the normal and faulty insulators are mostly the same, with only minor differences. However, they were all correctly detected and classified. Thus it can be shown that the method provides a high training accuracy and has a strong ability to eliminate interference.

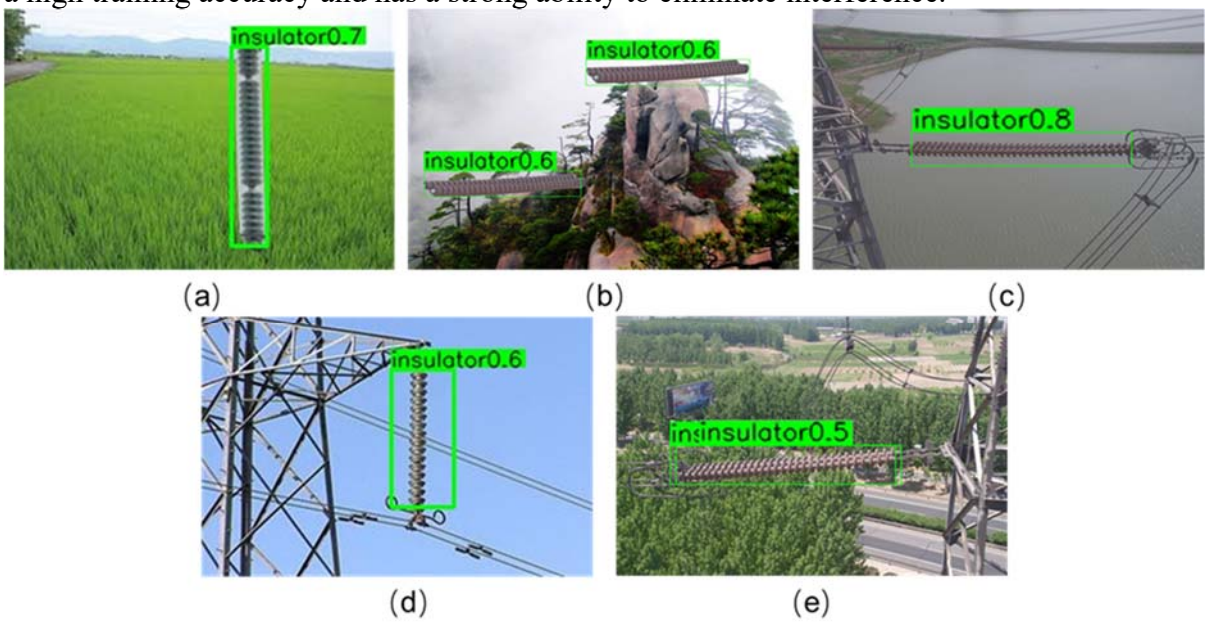

Figure 5. Detection results in different scenes. (a) Grass. (b) Mountain. (c) River. (d) High-voltage tower. (e) Tree.

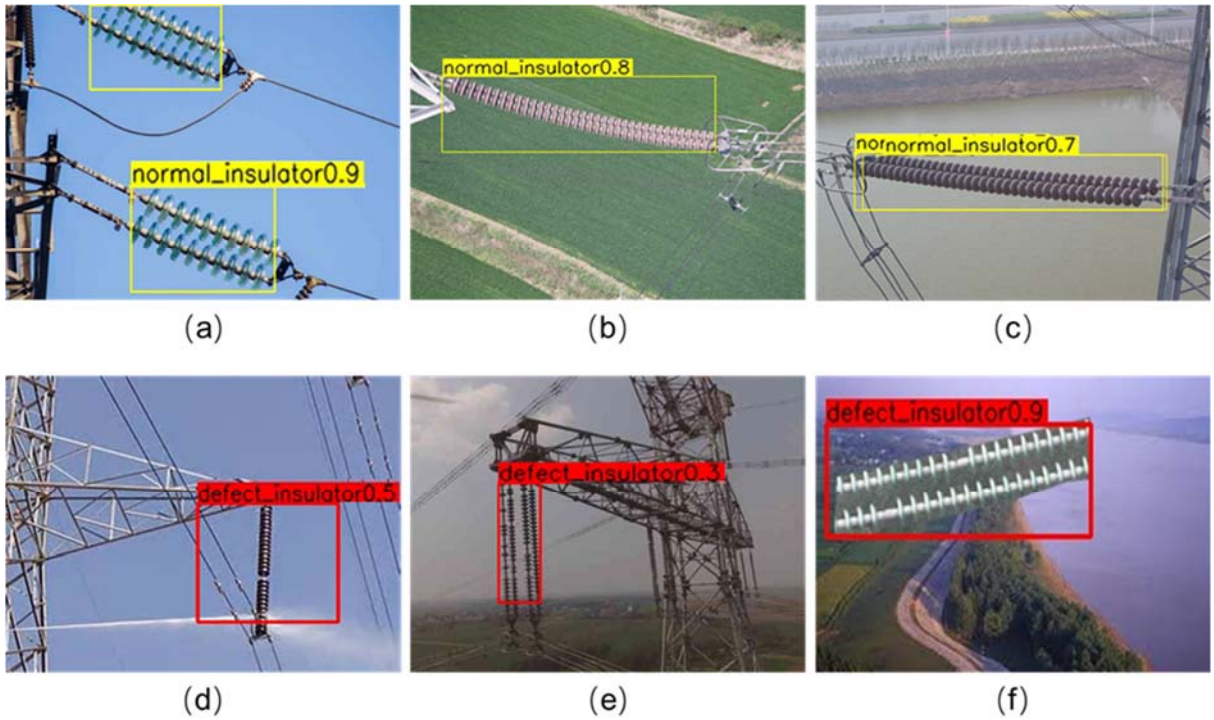

Figure 6. Insulator detection results. The normal insulators in (a) (b) and (c) are bounded by the yellow box; the defective insulators in (d) (e) and (f) are bounded by the red box. The confidence score and category are displayed above.

4. Conclusion

In this paper, an automatic insulator detection structure based on deep learning algorithms is presented. The SSD network is utilized to extract multi-scale features to localize the insulator from the aerial images captured by UAV, which effectively avoids the low efficiency of the traditional method based on regular intervals and handcrafted-feature. Moreover, the DenseNet is newly applied in the field of insulator inspection to classify the detected insulators. To overcome the scarcity of original images, both in quantity and background category, a fruitful data augmentation method is implemented. The results show that the insulator detection network and classification network can perform with the precision of 0.95 and 0.98 using the test dataset, respectively, which indicates that the proposed method can ensure the robustness and accuracy during the insulator detection. In the future, FPN (Feature Pyramid Network) will be considered for insulator inspection to achieve higher accuracy in more sophisticated situations.

References

[1] X. Tao, D. Zhang, Z. Wang, X. Liu, H. Zhang and D. Xu. (2020) "Detection of Power Line Insulator Defects Using Aerial Images Analyzed With Convolutional Neural Networks," in IEEE Transactions on Systems, Man, and Cybernetics: Systems, vol. 50, no. 4, pp. 1486-1498.

[2] V. N. Nguyen, R. Jenssen and D. Roverso. (2019) "Intelligent Monitoring and Inspection of Power Line Components Powered by UAVs and Deep Learning," in IEEE Power and Energy Technology Systems Journal, vol. 6, no. 1, pp. 11-21.

[3] X. Miao, X. Liu, J. Chen, S. Zhuang, J. Fan and H. Jiang. (2019) "Insulator Detection in Aerial Images for Transmission Line Inspection Using Single Shot Multibox Detector," in IEEE Access, vol. 7, pp. 9945-9956.

[4] H. Jiang, X. Qiu, J. Chen, X. Liu, X. Miao and S. Zhuang. (2019) "Insulator Fault Detection in Aerial Images Based on Ensemble Learning With Multi-Level Perception," in IEEE Access, vol. 7, pp. 61797-61810.

[5] Z. Zhao, N. Liu and L. Wang. (2015) "Localization of multiple insulators by orientation angle detection and binary shape prior knowledge," in IEEE Transactions on Dielectrics and Electrical Insulation, vol. 22, no. 6, pp. 3421-3428.

[6] W. Wang, Y. Wang, J. Han and Y. Liu. (2016) "Recognition and Drop-Off Detection of Insulator Based on Aerial Image," 2016 9th International Symposium on Computational Intelligence and Design (ISCID), Hangzhou, 2016, pp. 162-167.

[7] Q. Wu, J. An and B. Lin. (2012) "A Texture Segmentation Algorithm Based on PCA and Global Minimization Active Contour Model for Aerial Insulator Images," in IEEE Journal of Selected Topics in Applied Earth Observations and Remote Sensing, vol. 5, no. 5, pp. 1509-1518.

[8] X. Zhang, J. An and F. Chen. (2010) "A Simple Method of Tempered Glass Insulator Recognition from Airborne Image," 2010 International Conference on Optoelectronics and Image Processing, Haikou, pp. 127-130.

[9] M. Oberweger, A. Wendel, and H. Bischof. (2014) “Visual recognition and fault detection for power line insulators,” in Proc. 19th Comput. Vis. Win. Workshop, pp. 1–8.

[10] V. S. Murthy, K. Tarakanath, D. K. Mohanta and S. Gupta. (2010) "Insulator condition analysis for overhead distribution lines using combined wavelet support vector machine (SVM)," in IEEE Transactions on Dielectrics and Electrical Insulation, vol. 17, no. 1, pp. 89-99.

[11] Z. Zhao, G. Xu, Y. Qi, N. Liu and T. Zhang. (2016) "Multi-patch deep features for power line insulator status classification from aerial images," 2016 International Joint Conference on Neural Networks (IJCNN), Vancouver, BC, pp. 3187-3194.

[12] W. Liu, D. Anguelov, D. Erhan, C. Szegedy, S. Reed, C.-Y. Fu, and A. C. Berg. (2016) “Ssd: Single shot multibox detector,” in European conference on computer vision. Springer, pp. 21–37.

[13] K. He, X. Zhang, S. Ren, and J. Sun. (2016) “Deep residual learning for image recognition,” in Proceedings of the IEEE conference on computer vision and pattern recognition, pp. 770–778.

[14] S. C. Wong, A. Gatt, V. Stamatescu and M. D. McDonnell. (2016) "Understanding Data Augmentation for Classification: When to Warp?," 2016 International Conference on Digital Image Computing: Techniques and Applications (DICTA), Gold Coast, QLD, pp. 1-6.
[15] G. Huang, Z. Liu, L. van der Maaten and K. Q. Weinberger. (2017) "Densely connected convolutional networks", Proc. IEEE Conf. Comput. Vis. Pattern Recognit., pp. 4700-4708.